Improvement of Bearing Life through Bonding of Non-metallic Inclusions with Matrix*1

T. SADA Y. NONAKA T. MIKAMI K. KIZAWA

Non-metallic inclusions in the material of rolling bearings are well-known to induce subsurface initiated spalling. Among these inclusions, oxides in particular are believed to harm bearing life due to the weak adhesion between the oxide and the matrix. In this study, life tests were carried out for the inner rings of deep groove ball bearings made from low cleanliness bearing steel to which hot isostatic pressing (HIP) had been applied. From the experimental results, we confirmed that life improvement of radial bearings can be achieved by bonding the oxides with the matrix. Furthermore, void closing analyses were carried out using a model for ideal void shape. From the correlation between the void closing rates obtained by these analyses and the interface bonding rates measured for the inner rings, we found that void closing analysis is effective in predicting the state of the interface between the oxide and the matrix.

***Key Words**: rolling bearing, rolling contact fatigue, non-metallic inclusion, hot isostatic pressing, finite element analysis*

1. Introduction

Non-metallic inclusions in the material of rolling bearings are well-known to induce subsurface-initiated spalling. Among these inclusions, oxides are believed to be particularly detrimental to bearing life due to the weak bonding between the oxide and the matrix[1), 2)]. For this reason, Japanese steelmakers have established a technology to reduce the amount of oxygen, which generates oxides, in steel to the maximum extent possible, in order to achieve stable production of bearing steel with high cleanliness (meaning that inclusions are small and few)[3-5)]. However, looking around the world, bearing steel of such high cleanliness is not readily available. As such, if a technology which enabled a bearing made with low-cleanliness bearing steel to have a life equivalent to a bearing made with high-cleanliness bearing steel was established, it would be possible to manufacture high-quality bearings anywhere in the world.

Tsunekage and colleagues have published research results focused on the bonding of oxides and matrix as a factor other than cleanliness which affects the rolling contact fatigue (RCF) life of bearing steel[6), 7)]. Their research confirms that rolling contact fatigue life is improved using bearing steel in which oxides have been bonded with the matrix using hot isostatic pressing (HIP). This was verified in a thrust-type RCF test. In this type of test, the direction of the contact load relative to the steel bar rolling direction differs to radial bearings (e.g. deep groove ball bearings, which are the most common type of rolling bearing used). Moreover, although actual bearings are normally used under a contact load which will not result in the occurrence of plastic deformation, the thrust-type RCF test uses a large contact load at which plastic deformation will occur.

In this study, in order to confirm if bonding oxides to the matrix would be effective in increasing the life of an actual bearing, life tests with radial load were carried out for the inner rings of deep groove ball bearings made from low-cleanliness bearing steel to which hot isostatic pressing (HIP) had been applied. By comparing the lives of inner rings with three different levels of HIP processed steel, the pressurization condition necessary to obtain life equivalent to mass-produced bearings was clarified. Furthermore, the authors investigated a method of predicting the bonding state of oxides with the matrix by conducting an FEM analysis using a simple void model.

*1 *This paper was prepared based on Journal of Japanese Society of Tribologists No. 61 Vol. 4 (2016) 264-274.*

2. Life Test on the Effect of Pressurization

2. 1 Test Bearings

Inner rings of deep groove ball bearings (I.D.:30mm, O.D.: 62mm, width: 16mm - bearing no. 6206) made from low-cleanliness, high-carbon chrome bearing steel (JIS-SUJ2) with the oxygen content intentionally made high were produced. This steel was fabricated in a vacuum induction melting (VIM) furnace with a 100 kg capacity. The oxygen content of this steel was 27 ppm, which is high compared to the SUJ2 steel mass produced in Japan, which has an oxygen content of only a few ppm[8]. The inner rings were fabricated using the steel bars made by applying the three levels of HIP processing shown in **Table 1** (HIP) and the steel bar to which HIP had not been applied (non-HIP). These steel bars were normalized, annealed and then turned to achieve the inner ring shape. After this, the blanks were quenched and tempered, then grinded and given raceways with super finishing to manufacture the final inner rings using the same processes as mass production. The surface hardness of these inner rings ranged between 62 and 63 HRC. Finally, these inner rings were assembled with mass-produced outer rings, balls and retainers to form test bearings.

The HIP-2 shown in **Table 1** used practically the same conditions as the study by Tsunekage and colleagues in which rolling contact fatigue life was confirmed to have improved [6), 7)] (1 150℃, 147 MPa, 5 h) (the duration was shortened). HIP-3 had higher temperature conditions than HIP-2 and a pressure close to the upper limit of most HIP processing equipment (200 MPa)[9], while HIP-1 had the same pressure as HIP-2 but lower temperature. **Figure 1** shows an example for the temperature and pressure measured during HIP processing.

Table 1 HIP conditions

Condition	Temperature	Pressure	Duration
HIP-1	1 050℃	150 MPa	4 h
HIP-2	1 150℃	150 MPa	4 h
HIP-3	1 200℃	193 MPa	4 h

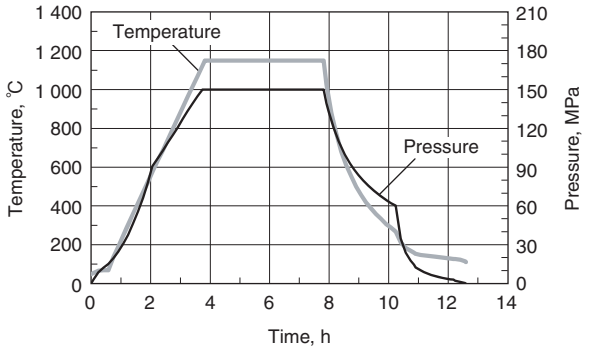

Fig. 1 Example of HIP processing log (HIP-2)

2. 2 Bonding State between Inclusions and Matrix

Figure 2 shows examples of oxides observed in the cross-sections of inner rings. All of the oxides observed are Al_2O_3 and the maximum diameter (circular equivalent diameter) in 8 600 mm^2 was predicted to be 14 μm in accordance with the extreme value statistics method[10]. Most of the oxides contained in the non-HIP inner ring had cavities between the matrix and the inclusion in the axial direction (longitudinal direction of the steel bar). Meanwhile, the majority of oxides in the HIP inner rings were bonded with the matrix. The bonding state was quantified in accordance with the following steps in order to elucidate difference in bonding states depending on the implementation or lack of HIP processing, and HIP processing conditions.

First, the authors used a non-metallic inclusion measurement device (METALSPECTOR II-C made by Toshiba Solutions) on the samples to detect the oxides in the cross-sections of the axial direction of the non-HIP and the three different HIP inner rings. Then, of the oxides with an equivalent circle diameter of 4 μm or greater detected in the four cross-sections of each inner ring (where each cross-section had an area of 34.32 mm^2), the largest fifty were made the subjects of this evaluation. Of the inclusions comprising of both oxides and sulfides, the researchers only used those where the cross-sectional area of the oxide was one-third or more of the overall compound inclusion's cross-sectional area. The existence of cavities in the individual oxides included in the evaluation was determined with an optical microscope and the interface bonding rate (%), as defined by the following equation, was calculated.

$$\text{Interface bonding rate} \equiv \frac{\text{No. of bonding inclusions}}{\text{Total no. of examined inclusions}} \times 100 \quad (1)$$

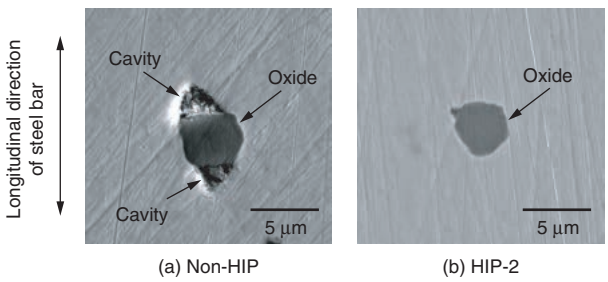

Fig. 2 Examples of observed oxides

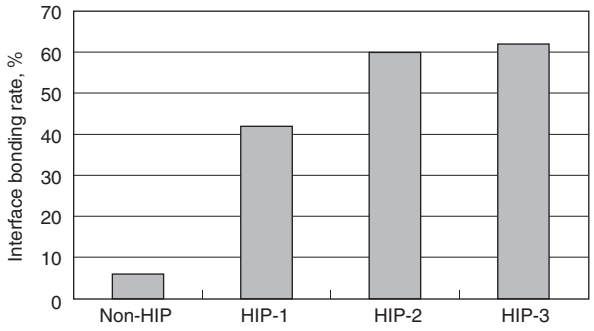

Fig. 3 Change in interface bonding rate of oxide according to the HIP process

Figure 3 shows the derived interface bonding rate. For the non-HIP inner ring, the interface bonding rate is 6%, meaning that there are cavities between the matrix for most oxides. If HIP processing is applied, the number of bonded inclusions increases and the bonding rate increases with the temperature and pressure. However, there was no clear difference in the bonding rates of HIP-2 and HIP-3.

2. 3 Life Test Method

Figure 4 is a schematic of the life test rig used for the life test. This test rig's structure is one whereby a radial load can be applied equally to four bearings and in the case of this test, the two inside bearings were established as the test bearings, while the two outside bearings were made support bearings. Bearings with long-life specifications were established as the support bearings so that the test bearings would be prioritized in regard to damage. The test rig was operated using the conditions

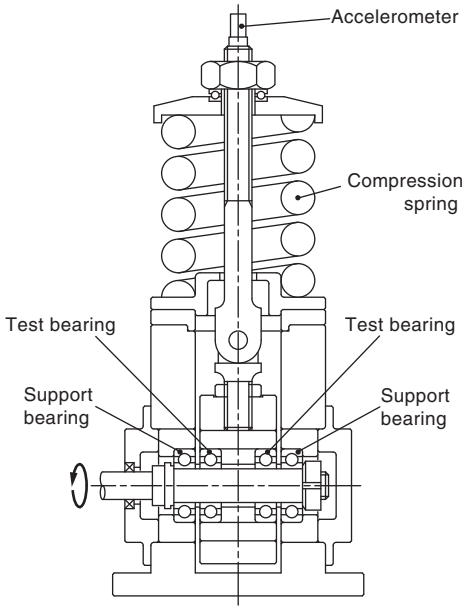

Fig. 4 Schematic diagram of life test rig

Table 2 Life test conditions

Radial load	9 000 N
Rotational speed	2 500 min^{-1} (inner ring)
Lubricant	Mineral oil (ISO-VG68)
Lubrication	Oil circulation with on-line filter (Nominal filtration rating : 2 μm)
Operating temperature	65 ± 5℃

shown in **Table 2**, and spalling occurrence was detected using the accelerometer mounted on its top. The test conditions were set so that sufficient lubricant film would form in order to ensure the occurrence of subsurface-initiated spalling. The bearing temperature was made 65℃, and, using the procedures shown in the appendix of reference 11), the lubricant film parameter at the contact between ball and inner race was 4.5. The life test was conducted five times for each bearing steel condition (non-HIP, HIP-1, HIP-2 and HIP-3); as two bearings per test are investigated, 10 bearing of each type were tested.

2. 4 Target Life

The aim of this study was to raise the life of a bearing made with low-cleanliness steel to that equivalent to a mass-production bearing made with high-cleanliness steel. For that reason, the actual capability of a mass-production bearing is used as the target life. The life of a mass-production bearing under the conditions shown in **Table 2** is almost ten times that of basic rating life, however this test only considers the inner ring, therefore the basic rating life of the inner ring was calculated and ten times this figure was set as the target life.

The basic dynamic load rating of inner ring 6206 calculated by ISO 281[12] and ISO/TR 1281-1[13], is 20 070 N. Based on this, the basic rating life of the inner ring under the conditions shown in **Table 2** will be 73.9 hours. This result multiplied by ten gives 739 hours, therefore this was used as the target life for the inner ring made with low-cleanliness steel.

2. 5 Life Test Results

Figure 5 is a Weibull distribution plot of the life test results. As this test only focuses on the inner ring, the test was suspended if spalling occurred on any other part of the bearing and the data taken up until that point was made suspended data. From their appearance, all of the spalling that occurred in the inner ring was judged to have been initiated from subsurface of the raceway. For the non-HIP inner ring, spalling occurred on the three tests, therefore the median ranks of the spalling data was determined in consideration of two suspended data[14] and the population was estimated. Meanwhile, for the HIP inner ring tests, spalling only occurred once

for all three HIP levels when the test was conducted for 3 000 hours therefore it was determined difficult to obtain anymore spalling data and the tests were suspended when operating time exceeded fifty times the basic rating life of the bearing (3 390 hours). As such, it was not possible to use linear regression of the spalling data to estimate the population, therefore linear regression was applied to five points of all data, including the suspended data, to estimate the population for the sake of convenience.

Table 3 shows the lives (L_{10iE}) of the inner rings with 90% reliability of each estimated population. Neither the non-HIP nor the HIP-1 inner ring reached the target life. Meanwhile, the HIP-2 inner ring, which had the same conditions applied as that used by Tsunekage and colleagues, and the HIP-3 inner ring, which was treated at the highest pressure, achieved four times the target life, clearly demonstrating that the life had been improved.

The above results verified that HIP processing could improve bearing life on radial bearings in the same way as it had been confirmed in thrust-type RCF tests. Moreover, by making the inclusions in the material bond with the matrix, the life of a bearing made with low-cleanliness steel can be made equivalent to a bearing manufactured with high-cleanliness steel.

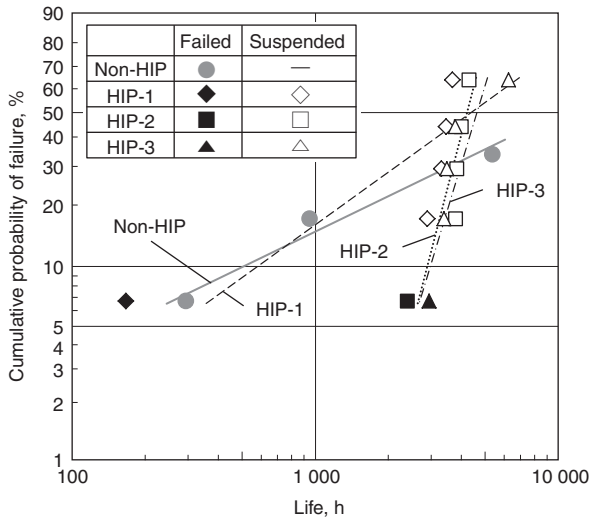

Fig. 5 Life test results of inner rings

Table 3 Estimated lives of inner rings

Specimen	L_{10iE}, h
Non-HIP	504.4
HIP-1	577.0
HIP-2	2 894.4
HIP-3	2 977.6

3. Void Closing Analysis Using FEM

An analysis was conducted using the finite element method (FEM) aimed at a more detailed investigation of the relationship between the HIP processing conditions and the state of oxide interface bonding mentioned in the previous section (**Fig. 3**). However, a model which only had voids in the material was adopted in order to simplify the phenomenon as much as possible. Because the actual internal conditions of the cavities in the material are unknown (whether they are full of some type of gas or entirely empty) for the analysis of this study, it was assumed that pressure did not occur inside the void even if the material was subjected to compressive stress.

As seen in **Fig. 1**, HIP processing involves increasing both temperature and pressure simultaneously, meaning that material strength will reduce and deformation will occur. Moreover, temperature increase will lead to phase transformation. In order to reflect these complex phenomena, a heat treatment simulation software (DEFORM-HT) was used for the analysis.

3. 1 Analysis Conditions

Figure 6 shows the void closing analysis model. The shape of the void located in the middle of the area was defined as a cosine shape with Equation (2) so that it would simulate a cavity when the material was stretched in the rolling direction.

$$y = \pm \frac{1}{4} \cos\left(\frac{\pi}{2} x\right) \quad (2)$$

The temperature and pressure combinations shown in **Table 4** were applied in the analysis of void deformation accompanying HIP processing. The conditions given in the table for HIP-1, HIP-2 and HIP-3 are equivalent to the HIP processing applied to the inner rings material used for the life test described in the previous section. HIP-3 pressure was 193 MPa according to the actual processing log, however it is approximated as 200 MPa in order to position at equal intervals for ease of analysis.

Because it is necessary to assume the changes in temperature and pressure inputted in the analysis against conditions with no processing results, the researchers first prepared a model of the actual processing log, as shown in the example provided in **Fig. 7**. For the temperature and pressure increase phase and holding phase the interval between critical points of the temperature and pressure in the processing log respectively were approximated using a straight line. For the temperature and pressure drop phase, the interval between each critical point was approximated with a catenary, except for the final stage of the pressure drop which was approximated with a parabola.

For the purposes of this analysis, creep brought on by holding at high temperature is not taken into consideration, therefore the duration is shortened. Moreover, in the model shown in **Fig. 6**, the size of the voids relative to the area are bigger than the actual cavities around the inclusions in the material therefore pressure is corrected by multiplying a coefficient determined in a pre-analysis. Based on the processing log of the three HIP levels applied to the inner rings for the life tests of **Section 2**, the conditions with no processing results were determined through either interpolation or extrapolation of the critical points and input data was created by connecting the interval of each critical point in the abovementioned model.

In regards to the elastic-plastic property of the material dependent on temperature, a database prepared by the Research Group on Database of Cooling Power of Quenchant affiliated with the Japan Society for Heat Treatment focused on the cooling performance of quenching coolant[15), 16)] was used. The linear hardening rule of Equation (3) was applied to the flow stress, σ, which expresses plastic behavior. However, in the abovementioned database, yield stress, σ_y, and the strain hardening coefficient, H', are not defined at temperatures exceeding 900℃; therefore for the purposes of this analysis, these values were extrapolated based on data up to the maximum temperature of 1 200℃.

$$\bar{\sigma} = \sigma_y + H'\bar{\varepsilon} \tag{3}$$

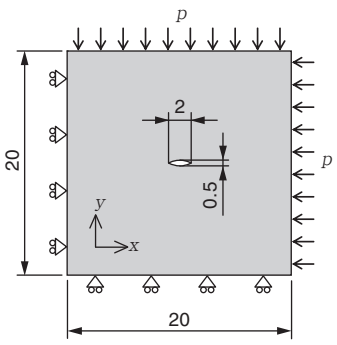

Fig. 6 Plane strain model for void closing analysis

Table 4 Parameters for void closing analysis

Temperature / Pressure	1 050℃	1 100℃	1 150℃	1 200℃
100 MPa	*	*	*	*
150 MPa	*HIP-1	*	*HIP-2	*
200 MPa	*	*	*	*HIP-3

* : Analyzed conditions.
HIP-1 to 3 : Equivalent to the conditions applied to the test bearings

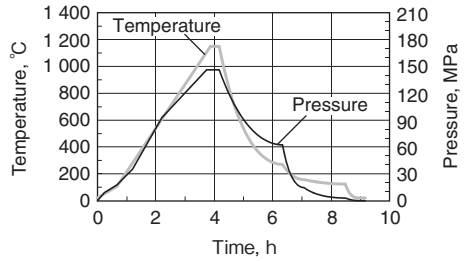

Fig. 7 Example of modeled HIP processing log (1 150℃, 150 MPa)

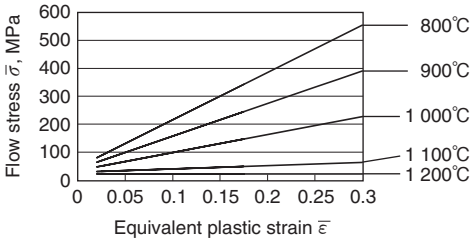

Fig. 8 Relationship between equivalent plastic strain and flow stress for each temperature

Here, $\bar{\varepsilon}$ is equivalent plastic strain. **Figure 8** shows the relationship between equivalent plastic strain and flow stress at temperatures of 800℃ or higher.

3. 2 Analysis Results

Figure 9 shows examples of void deformation caused by HIP processing as obtained through the analysis. It can be seen that the voids after HIP has been applied are smaller than pre-HIP. In order to compare the degree of void deformation under each processing condition, the opening width, b, of the void's y direction (refer to **Fig. 10**) was made the characteristic dimension of a void and the void closing rate (%) was defined using Equation (4).

$$\text{Void closing rate} \equiv \left(1 - \frac{b_{\text{Post-processing}}}{b_{\text{Pre-processing}}}\right) \times 100 \tag{4}$$

Figure 11 shows the void closing rates for each combination of temperature and pressure shown in **Table 4**, as obtained in the analysis. While it goes without saying, the closing rate increases as pressure and temperature increase.

Figure 12 shows the relationship between void closing rate obtained in the analysis and the measured interface bonding rate (**Fig. 3**) relative to the three HIP processing levels applied to the inner rings for the life tests of **Section 2**. The void closing rate of the non-HIP material has also been plotted in the figure as zero. The figure shows there is correlation between the void closing rate

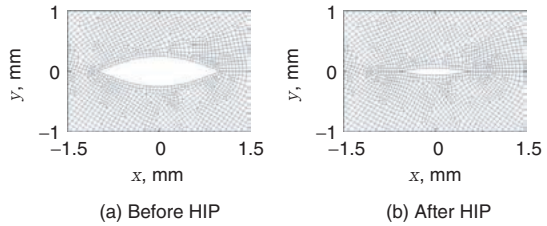

Fig. 9 Change in void shape due to HIP processing (1 050℃, 200 MPa)

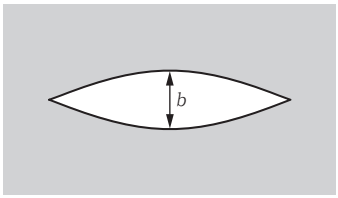

Fig. 10 Characteristic dimension of cosine-shaped void

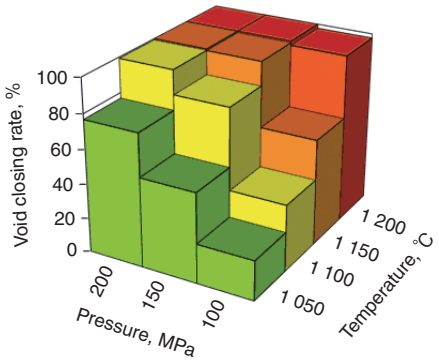

Fig. 11 Void closing rate for each HIP condition

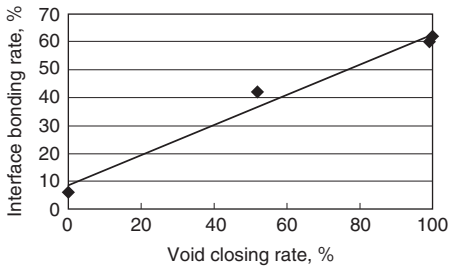

Fig. 12 Relationship between void closing rate and interface bonding rate

and interface bonding rate. The interface bonding rate, which expresses the percentage of the 50 inclusions being assessed that are bonded to the interface with the matrix, and the void closing rate, which expresses deformation relative to a schematically simple void, are related to two different phenomena. Despite this, due to the fact that correlation between these two was recognized, it can be considered that they are both indicators of how easily a cavity or void "collapses" relative to the degree of compressive stress and that their behavior under pressurization conditions is qualitatively consistent. Consequently, it is believed possible to relatively predict the bonding state of the inclusions which actually exist in the material with the matrix through a void closing analysis, as discussed in this section.

4. Conclusion

In this study, life tests were performed on inner rings of deep groove ball bearings made from steel with a high oxide content which had been subjected to three different levels of HIP processing. The result of these tests showed that service life could be improved even in radial bearings, just as it had been confirmed in thrust-type RCF tests, which differed in respect to load level and direction. Moreover, this study also confirmed that the degree of inclusion and matrix bonding differed depending on HIP processing conditions (temperature and pressure) and that this, in turn, affected service life. It can be deemed that the necessary pressure conditions to raise the life of a bearing made with low-cleanliness bearing steel to that of a mass-production bearing are 1 150℃ and 150 MPa.

Using a cosine-shaped void model, a coupled analysis of heat, phase transformation and elastic-plastic deformation was conducted. A correlation was recognized between the interface bonding rate measured on the inner rings using a life test (percentage of inclusions bonded with the matrix) and the void closing rate obtained through the analysis (extent to which the void is closed). Therefore, it was clarified that this analysis is effective in predicting the bonding state of inclusions and matrix.

References

1) T. Uesugi: Recent Development of Bearing Steel in Japan, Tetsu-to-Hagané, Vol. 74, No. 10 (1988) 1889 (in Japanese).
2) T. Udagawa, K. Suga, T. Kozuka, T. Nishikawa: The Influence of the Non-metallic Inclusions on the Rolling Contact Fatigue Damage Behavior of Bearing Steel, Aichi Steel technical review, Vol. 30, No. 1 (2013) 29 (in Japanese).

3) J. Nakashima, T. Toh: Improvement of Continuously Cast Slabs Quality by Decreasing of Nonmetallic Inclusions, NIPPON STEEL TECHNICAL REPORT, No. 104 (2013) 42.
4) T. Emi: Steelmaking Technology for the Last 100 Years: Toward Highly Efficient Mass-Production Systems for High-Quality Steels, Tetsu-to-Hagané, Vol. 100, No. 1 (2014) 31 (in Japanese).
5) K. Semura, H. Matsuura: Past Development and Future Prospects of Secondary Refining Technology, Tetsu-to-Hagané, Vol. 100, No. 4 (2014) 456 (in Japanese).
6) N. Tsunekage, K. Hashimoto, T. Fujimatsu, K. Hiraoka: Initiation Behavior of Crack Originated from Non-Metallic Inclusion in Rolling Contact Fatigue, Sanyo Technical Report, Vol. 18, No. 1 (2011) 23 (in Japanese).
7) K. Hashimoto, T. Fujimatsu, N. Tsunekage, K. Hiraoka, K. Kida, E. C. Santos: Effect of inclusion/matrix interface cavities on internal-fracture-type rolling contact fatigue life, Materials and Design, Vol. 32, No. 10 (2011) 4980.
8) K. Kawakami: Generation Mechanisms of Non-Metallic Inclusions in High-Cleanliness Steel, Sanyo Technical Report, Vol. 14, No. 1 (2007) 22 (in Japanese).
9) T. Nakai: Recent Trend in HIP Technology, JOURNAL OF THE JAPAN WELDING SOCIETY, Vol. 65, No. 8 (1996) 622 (in Japanese).
10) K. Kizawa, M. Gotoh: Estimation of Rolling Contact Fatigue Life through Evaluation of Cleanliness in Bearing Steel, Koyo Engineering Journal English Edition, No. 163E (2003) 37.
11) Technical Committee on Life of Rolling Bearings: Life Test Manual for Rolling Bearings (Part 3), Journal of Japanese Society of Tribologists, Vol. 53, No. 5 (2008) 326 (in Japanese).
12) ISO 281:2007, Rolling bearings - Dynamic load ratings and rating life.
13) ISO/TR 1281-1:2008, Rolling bearings - Explanatory notes on ISO 281 - Part 1: Basic dynamic load rating and basic rating life.
14) L. G. Johnson: The Statistical Treatment of Fatigue Experiments, Elsevier (1964).
15) M. Narazaki: Present State and Scope on Heat Treatment Simulation, NETSUSHORI, Vol. 50, No. 4 (2010) 343 (in Japanese).
16) Y. Watanabe: SOKEIZAI, Vol. 55, No. 2 (2014) 42 (in Japanese).

T. SADA*

Y. NONAKA**

T. MIKAMI*

K. KIZAWA*

* *Material R&D Dept., Research & Development Headquarters*
** *Heat treatment Production Engineering Dept., Production Engineering Headquarters*